SAND79-0377
Unlimited Release
UC-37

Borehole-Inclusion Stressmeter Measurements in Bedded Salt

C. Wayne Cook, Edward S. Ames

BOREHOLE-INCLUSION STRESSMETER MEASUREMENTS IN BEDDED SALT*

by C. W. Cook and E. S. Ames,
Sandia National Laboratories, Albuquerque, NM 87185

ABSTRACT

Sandia purchased borehole-inclusion stressmeters from a commercial supplier to measure in situ stress changes in bedded salt. However, the supplied stressmeters were difficult to set in place and gave erratic results in bedded salt. These problems were overcome with a new extended platen design. Also a straingaged transducer was designed which can be read with a conventional data logger.

Due to the nonlinear behavior of bedded salt under uniaxial loading, a new empirical calibration scheme was devised. In essence, the stressmeters are calibrated as force transducers and this calibration curve is then used to determine the relationship between uniaxial stress imposed in bedded salt and the gage's output.

The stressmeter and calibration procedures have been applied under mine conditions and produced viable results.

Future work will involve finite element analysis to calculate the observed behavior of the stressmeters. The response of the stressmeters in bedded salt is neither that of a true stressmeter or of a true strainmeter. However, repeatable calibrations make the gages very useful.

---

*This work was supported by the United States Department of Energy.

TABLE OF CONTENTS

LIST OF FIGURES

INTRODUCTION

In conjunction with the planning for the Waste Isolation Pilot Plant (WIPP) which may be located near Carlsbad, New Mexico, the need was recognized for a stressmeter to monitor stress changes in bedded salt. During construction of the WIPP facility, in situ stress changes will be monitored to verify code predictions and to certify structural integrity. To meet the WIPP requirements, several vibrating-wire stressmeters (VWS) with soft-rock platens were purchased from IRAD Gage, Inc., Lebanon, NH. The principle of operation of the VWS is to wedge (preload) a cylinder, which has a pretensioned wire stretched diametrically across its bore, into a borehole. By calibration, stress changes in the rock are related to the period of oscillation of the pretensioned wire.[1] Since no calibration data was available for the VWS in bedded salt, large blocks of bedded salt were obtained from the Mississippi Chemical Company potash mine in southeast New Mexico for the purpose of running calibration tests.

Following the conventional calibration procedures,[1] the VWSs were calibrated in 46 x 46 x 30-centimeter (cm) blocks of bedded salt in a universal testing machine. These initial uniaxial calibrations presented two problems:

1. It was difficult to set the gages at the recommended preload, and

2. The results were erratic and not repeatable.

To better understand these problems, the VWS and bedded salt were investigated separately. This paper discusses the stress-strain characteristics of bedded salt, a new platen design to solve the setting problem, a new stressmeter design, a new calibration technique, and the field trial results of these new approaches.

The primary intent of this paper is to describe the characteristics of the newly developed borehole-inclusion stressmeters. All rock tests were run in bedded salt. An explanation of the behavior of bedded salt under various loading conditions is beyond the scope of this paper.

Stress-Strain Characteristics of Bedded Salt

After consulting with W. Wawersik,[2] the type of tests that should be performed in order to better understand the behavior of bedded salt was decided upon. Data were obtained from a series of uniaxial loading tests in which stress-strain curves were generated. Loading and unloading were recorded from repeated cycles. Specially designed extensometers with a 30.5-cm span were mounted directly on the salt blocks. Linear variable displacement transformers (LVDT) were used to measure the strain, and the calibrated input of the universal testing machine was used to determine the uniaxial stress level.

The data from three different salt blocks are shown in Figure 1. Block I was run through four cycles. Runs 1 and 2 had a maximum input of 12.7 megapascals (MPa) and runs 3 and 4 had a maximum input of 19.3 MPa. Note that each succeeding loading tended to follow the preceding unloading. On run 3 the input was held at 19.3 MPa for 8 minutes. During this time the strain increased by 1200 microstrain but a stressmeter in the same block did not show a change in its reading. The data from Blocks II and III are included to show the variations obtained from different blocks. The variations seen are within $\pm$ 5 percent, which is reasonable for different rock samples.

Figure 1 shows that the stress-strain curve for bedded salt is nonlinear and exhibits a large hysteresis. From this data it was concluded that a meaningful calibration of a stressmeter would have to be obtained on the first loading cycle. Under mine conditions an increase in the in situ stress is the normal occurrence as mining progresses.

IRAD VWS Platen Redesign

The difficulties encountered in setting the VWS with soft rock platens (Figure 2) seemed to be caused by the gage's stiffness. As supplied, the platens tended to embed themselves in the salt at the recommended preload. To eliminate this problem the area of the platens had to be increased and/or the stiffness of the gage reduced.

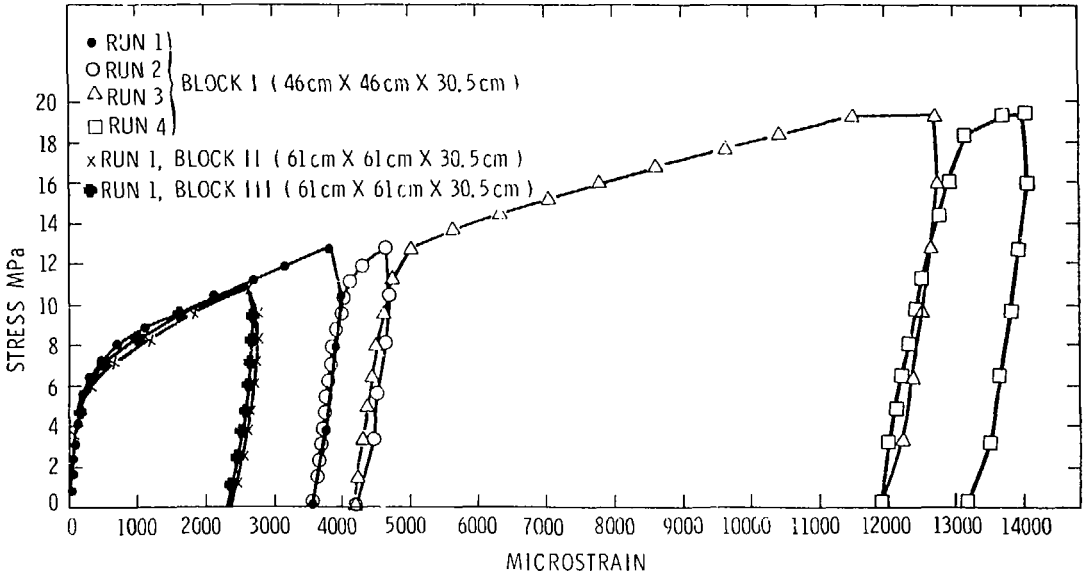

STRESS VERSUS STRAIN FOR THREE SALT BLOCKS

Fig. 1

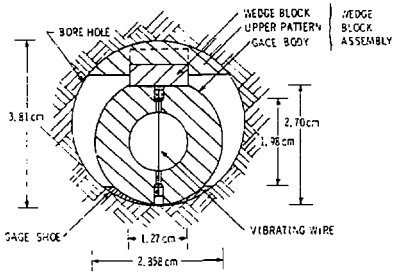

Fig. 2. Cross-sectional view of a VWS in a borehole

No attempt was made to redesign the basic VWS which appeared to be a durable, reliable transducer. However, the way in which the platens apply loading to the transducer was investigated with the SANDIA-BMINES computer program which uses the finite element method.[3] A complete description of the modeling technique used is contained in Reference 3. This study pointed out two significant points:

1. The stiffness of the gage is strongly dependent on the angle through which the body of the gage is loaded. As supplied (Figure 2), the bottom platen (gage shoe) loads the gage through a 120 degree angle and the top of the gage is loaded across the flat of the wedge. This arrangement gives a theoretical gage stiffness of 16.3 N/m x 10^{-8}. Decreasing the loading angle of the gage shoe to a line load gives a stiffness of 9.6 N/m x 10^{-8}, or a decrease in stiffness of 41 percent.

2. The study pointed out that the calculated gage stiffness depends on the portion of the gage that is used as a reference. The above stiffness values are referenced to the outer surface of the VWS cylinder. If the gage stiffness is based on the change in diameter of the cylinder bore, a 25 percent increase in stiffness results.

Laboratory experiments were performed to verify the theoretical predictions and the results are shown in Figure 3. The upper two curves were run with the VWS in a press with the top of the gage loaded across the cylinder flat and the bottom of the gage in a lucite block. The lucite block simulated the bottom half of a 3.8-cm borehole. Decreasing the width of the bottom platen from 3.05 cm to 1.27 cm resulted in a decrease in gage stiffness of roughly 39 percent. The lower curve was an attempt to simulate a line load on the top and bottom of the gage. This configuration resulted in the least stiffness.

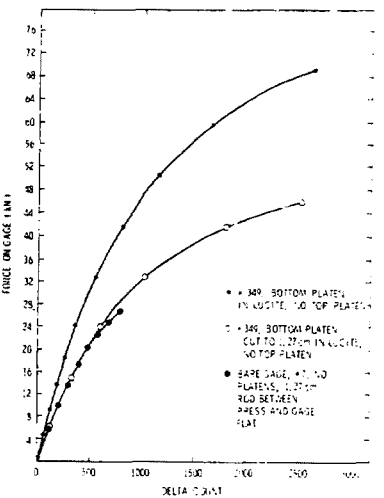

Fig. 3 – VWS Sensitivity variations for three loading conditions.

Using the above results, new platens were designed to provide a line load on the top and bottom of the gage. The new platens were also lengthened so they would contact more of the borehole's surface. Extending the platens beyond the gage body necessitated making them thicker so that the stressmeter would be the weakest part of the assembly.

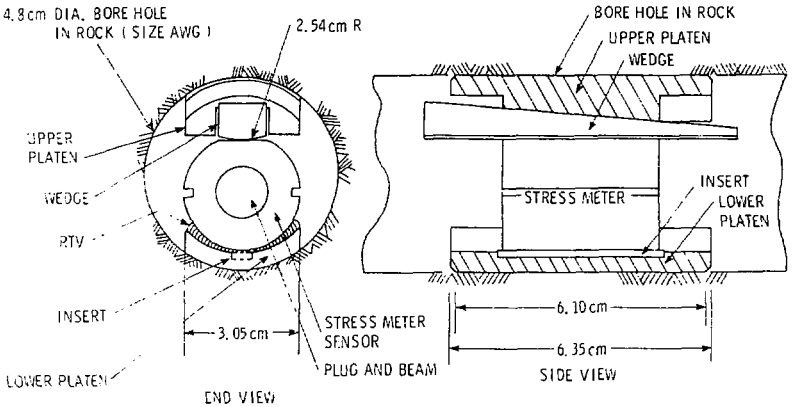

Fig. 4 – Extended platen design.

Figure 4 is a drawing of the extended platen design. The sensor shown is a straingaged stressmeter which is described in the following section. The extended platen can be approximated by a cantilever beam of rectangular cross-section. Equation (1) gives the deflection of a cantilever beam for a uniformly distributed load.[4]

$$\delta = \frac{\omega \ell^4}{8EI} \qquad (1)$$

where

δ = deflection, m
w = load, N/m
ℓ = length, m
E = modulus of elasticity, N/m^2
I = moment of inertia, m^4 .

Theoretically, the gage stiffness was shown to be 9.6 N/m x 10^{-8}. Each extended platen supports 19 percent of the total load on the transducer. The stiffness of the extended platen (0.51-cm thick, 3.05-cm wide, 1.14-cm long) calculated from Equation (1), and with F = 2.07 x 10^{11} N/m^2, ℓ = 0.114 m, and I = 3.37 x 10^{-10} m^4, is 3.77 N/m x 10^{-8}. Considering the load supported by the extended platen, the overall result is that the platen is 2.07 times stiffer than the vibrating-wire transducer.

The results of the many tests run with the new platen design indicate that the platen stiffness is adequate.

Design of New Rigid Inclusion Stressmeter

The IRAD-supplied VWS requires a special data logger to read its output. A stressmeter whose output could be read with a conventional data logger was preferred, and a new borehole-inclusion stressmeter was designed to this end.

Available straingages and bonding cements indicated that a transducer could be designed using existing technology. The design of the straingaged stressmeter (SGS) is shown in Figure 5. Basically, the transducer consists of an outer body with an exterior shape identical to the VWS except for two grooves down the sides. The body has a bore with a Morse taper to accept the instrumented plug. Four alloy grid straingages (gage factor of 2.05) with a thermal coefficient of expansion matched to the brass plug are mounted on the beam section of the plug. Two of the straingages read the compression of the plug and the other two provide temperature compensation

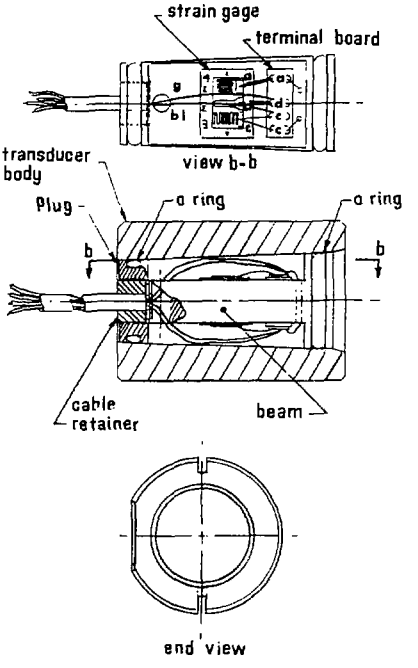

DRAWING OF SGS TRANSDUCER

Fig. 5

for the Wheatstone bridge configuration. The side grooves are sized so that the stiffness of the complete transducer essentially matches the stiffness of an IRAD VWS.

An unloaded SGS was temperature cycled in an oven. Over a temperature range of 21°C to 205°C the output with 18 Vdc excitation varies less than ± 0.6 millivolts (mV). This is equivalent to ± 0.8 MPa (± 115 psi) stress change in bedded salt. The calibration of the stressmeters in bedded salt is discussed in the section entitled "Uniaxial Stress Calibrations in Bedded Salt."

A common concern in using cemented straingages for longterm readings is creep of the cement bond. To check the stability of the SGS with extended platens a unit was wedged in an aluminum block at more than three times the normal preload. The total creep after 75 days was less than 0.6 percent.

After the development of SGS, both the SGS and the VWS were included in all subsequent laboratory and field testing.

Split Block Calibration

In the past, experimenters have attempted to determine the uniaxial sensitivity factor of borehole-inclusion stressmeters with respect to Young's modulus for the rock being monitored.[1,5,6] Since bedded salt does not have a constant Young's modulus (Figure 1), this approach was not used. A new approach was selected to calibrate the VWS and SGS in bedded salt.

First, by using a specially designed split block, the authors established a force-versus-output curve for each gage (including platens and setting wedge) (Figure 6). With the gage mounted in the split block, a universal testing machine was used to apply known forces on the assembly.

Figure 7 shows typical calibration curves for the VWS and SGS. Enough scatter (± 23 percent) was found between "identical" gages to justify individual calibrations. Using the Sandia interactive statistical package

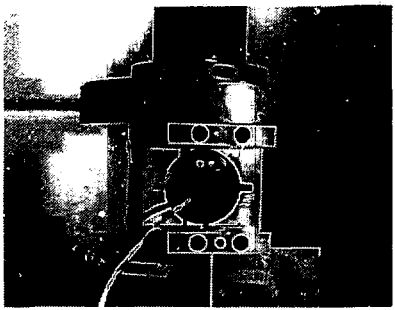

Fig. 6 – Split block calibration fixture

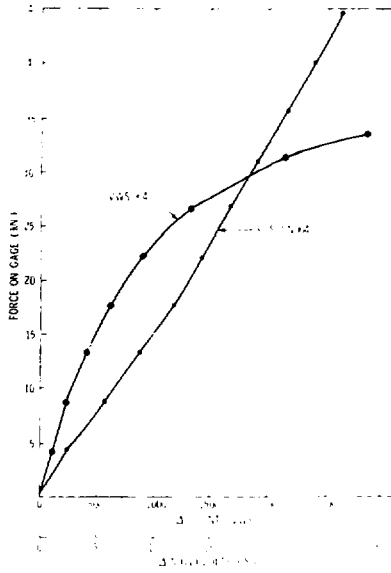

Fig. 7 – Typical block calibration cures for the VSW and SGS.

STATLIB,[7] least squares multiple regression analysis was used to fit polynominals to the split block data. The fit for the WWS curve shown in Figure 7 is given by Equation (2).

$$F = 228.67 + 39.903x\Delta C - 2.074E{-}2\ (\Delta C)^2 + 4.0707E{-}6\ (\Delta C)^3 \quad (2)$$

where

F = force, N

ΔC = count .

Similarly, the SGS curve in Figure 7 was fitted with Equations (3a) and (3b).

$$F = 41.93 + 2016.5(\Delta V) - 121.\ (\Delta V)^2 + 6.252(\Delta V)^3 \quad (3a)$$

for

$$\Delta V < 10\ mV$$

where

F = force, N
ΔV = delta voltage, mV .

$$F = -3453.1 + 1741.5(\Delta V) \quad (3b)$$

for

$$\Delta V \geq 10\ mV$$

where

F = force, N
ΔV = delta voltage, mV .

From these equations it is easy to determine the preload setting force and any subsequent force on the gage due to changes in the rock stress. Repeated split-block calibrations on an SGS, which was removed from the split block after each run, indicated that each point was repeatable to within $\pm$ 0.3 mV.

An empirical approach was used to relate the force on the stressmeter to changes in rock stress. These tests are described in the following section.

Uniaxial Stress Calibrations in Bedded Salt

The test equipment that was available for loading salt blocks dictated that two opposite faces be loaded while the remaining surfaces stayed free. With this type of test setup, the salt blocks were made as large as possible while the capability of 13 MPa stress changes in a 2.7-meganewtons (MN) universal testing machine was maintained. The 61 x 61 x 30.5-cm blocks with a 4.78-cm borehole in the center of the large face kept the free surfaces 12.8 radii from the borehole. To provide data on block size effects, 15.2 x 15.2 x 12.6-cm blocks were also used for calibration. Figure 8a shows the large block test setup and 8b shows the small block test setup.

The change in force on the stressmeter versus input stress changes is shown in Figure 9 (VWS) and Figure 10 (SGS). The change in force on the stressmeters was determined by using the gage output and the split-block calibration data. Input stress was obtained from the calibrated input force read on the universal testing machine divided by the area loaded.

The data from the SGS fall in a tighter band but the spreads seen on the VWS are reasonable for different rock samples. Notice that there is little difference between the small and large block calibration curves. Figure 9 includes the unloading curve for large Block II. Once the knee of the calibration curve (6-7 MPa) has been exceeded, the unloading curve deviates from the loading curve.

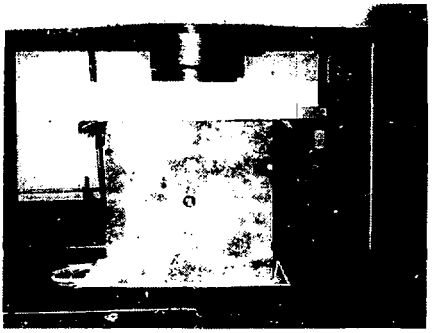

(a) - Large block test setups.

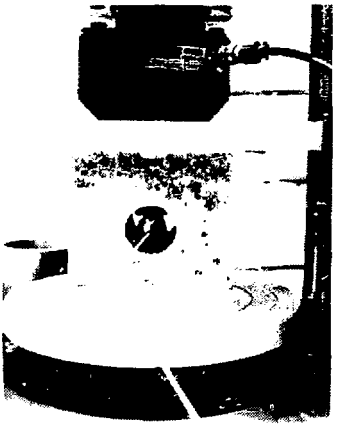

(b) - Small block test setups.

Fig. 8 - Blocks of salt used for uniaxial stress calibration

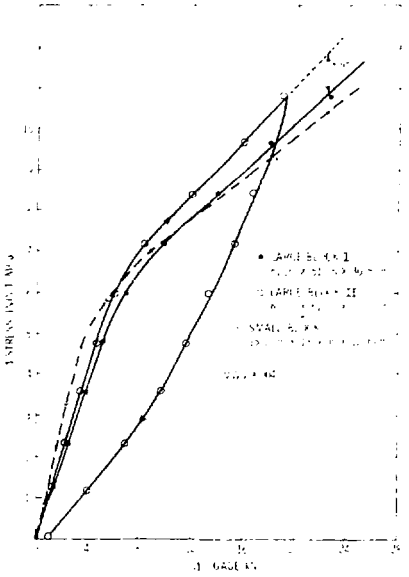

Fig. 9 - Delta force on VSW versus changes in salt.

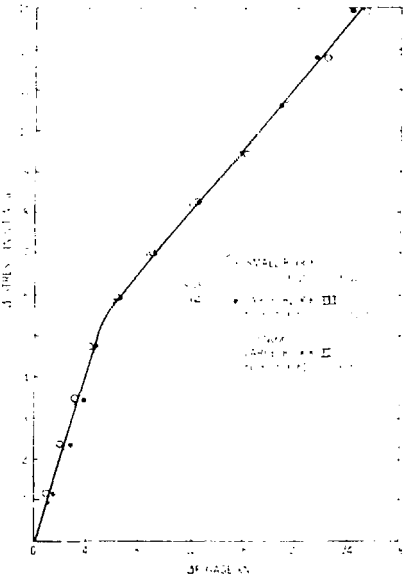

Fig. 10 - Delta force on SGS versus changes in salt.

By comparing Figures 9 and 10, it can be seen that the VWS large block data essentially include the SGS data. Based on this observation, the calibration curve for stressmeters was taken from the SGS data (SN004 and SN006 not shown) recorded on large Block III. Two straight lines were used to fit the data. These straight lines, which were determined by least squares with multiple readings, are given in Equation (4) below.

$$MPa = 0.9345(\Delta F) \tag{4a}$$

for

$$\Delta F < 6.16 \text{ kilonewtons (kN)}$$

where

MPa = stress change in bedded salt
F = force change on gage, kN

$$MPa = 3.463 + 0.3727(\Delta F) \tag{4b}$$

for

$$\Delta F \geq 6.16 \text{ kN}$$

where

MPa = stress change in bedded salt
ΔF = force change on gage, kN .

The preceding sections described how the stressmeter calibration data for bedded salt were obtained. To implement the calibration data the following procedure is used:

1. A least-squares multiple regression curve is fit to force-versus-gage output curve (Figure 7).

2. Similarly, a curve is fit to the stress-versus gage-force curve (Figure 10).

3. The initial setting force (~ 6.5 kN) is subtracted from all subsequent readings so that changes in stress are indicated.

4. The above curves are incorporated in a computer code which calculates stress change for specific gage outputs.

Field Trial Mississippi Chemical Mine

Recently, VWSs and SGSs were installed in pillars in the Mississippi Chemical Company potash mine. The mining being monitored utilized a 90-percent extraction ratio. Therefore, as mining progressed, the remaining support pillars ultimately failed. In situ pillar stress changes due to the mining were successfully monitored until after pillar slabbing had occurred. The VWSs were recorded manually once a day, and the SGSs were monitored hourly on a conventional data logger. The data recorded by SGS, SN002, and VWS, No. 349, are shown in Figure 11. Good agreement was obtained between the VWS and SGS. However, after the above VWS reached its maximum reading (count change of roughly 2200), a drop in stress was indicated. A corresponding drop did not occur in the SGS readings. In fact, the SGS output continued to rise until an induced stress change of 27.6 MPa was reached. The plateau seen on the SGS record corresponds to the time period during which the mining equipment was shut down for maintenance.

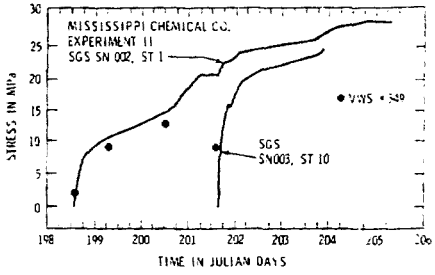

Fig. 11 – Mississippi Chemical Co. borehole-inclusion stressmeter data

Subsequent laboratory tests on the VWS duplicated the mine behavior when the input exceeded the range of the gage. The VWS with extended platens has a maximum range of 12-14 MPa. In other words, when the range of the VWS is exceeded an artifical drop in readings can occur. This behavior of the VWS is apparently due to the excitation of harmonics in the wire.

In the Mississippi Chemical Company experiment, an SGS, SN003, was installed in one pillar while a previously installed SGS, SN002, was indicating a stress change of 20.6 MPa. These data are also shown in Figure 11. SGS, SN003, shows a rapidly increasing stress change to a value approximately 14 percent below the reading on SGS, SN002. Cable failure occurred on SGS, SN003, at this point. The following section describes a laboratory experiment which investigates this behavior in prestressed salt.

Laboratory Investigation of Prestressed Salt

For this experiment a small salt block (15.5 x 15.2 x 12.7 cm) was preloaded to a stress of 6.78 MPa in a universal testing machine. An SGS was then set in the block. After 48 hours the input stress was increased to 9.04 MPa. Twenty-nine hours later the input stress was increased to 11.30 MPa. These results are shown in Figure 12. Observe that a behavior similar to the Mississippi Chemical Company experiment was obtained. Once the knee of the stress-strain curve for bedded salt (6-7 MPa) (Figure 1) is exceeded, the meter readings approach the in situ stress.

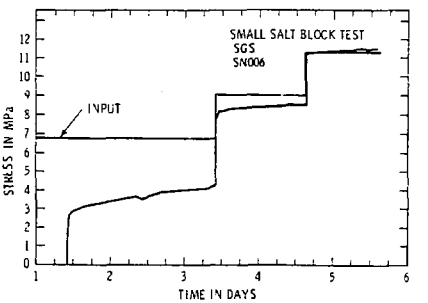

Fig. 12 - Data from laboratory investigation of prestressed salt

These results suggest another experiment. What will a borehole-inclusion meter read in bedded salt, which is seeing only the overburden? Plans are underway to perform this experiment sometime during 1979.

Summary and Conclusions

The new platen design described in this paper provides for easy installation and repeatable readings when borehole-inclusion stressmeters are used in bedded salt.

An SGS has been designed with sensitivity comparable to that of the VWS. The SGS also has a linear output, and a range that is at least three times as great as the vibrating wire unit; it can also be recorded on conventional data loggers.

An empirical approach was used to calibrate the inclusion stressmeters in bedded salt. Field trials using this approach produced results in bedded salt which appear viable.

The experiments run with the inclusion stressmeters and on bedded salt indicate that the stressmeters are neither a true stressmeter nor a true strainmeter. The shape of the calibration curve indicates that they are somewhat in between. During the salt-block calibrations it was found that under high constant loads (19.3 MPa) the strain readings increased while the stressmeter readings remained constant. Finite element techniques are planned to see if it is possible to calculate the observed behavior of the stressmeters in bedded salt.

It is hoped that the stressmeter technique discussed in this paper will provide reliable data which will permit code development and a better understanding of the behavior of bedded salt under various loading conditions.

References

1. I. Hawkes and W. V. Bailey, "Design, Develop, Fabricate, Test, and Demonstrate Permissible Low Cost Cylindrical Stress Gages and Associated Components Capable of Measuring Change of Stress as a Function of Time in Underground Coal Mines," USBM Contract Report (H0220050), November 1973.

2. Private communication, W. R. Wawersik, Sandia Laboratories, Albuquerque, NM.

3. J. R. Tillerson and M. M. Madsen, "Finite Element Simulation of a Vibrating Wire Stressmeter," Sandia Laboratories Report SAND79-0356, Albuquerque, NM (to be pulbished).

4. S. Timoshenko, Elements of Strength of Materials, D. Van Nostrand Co., Inc., New York, 1949, p. 185.

5. A. F. Fossum, J. E. Russell, and F. D. Hansen, "Analysis of a Vibrating-Wire Stress Gage in Soft Rock," Experimental Mechanics, 17, No. 7, 261-264 (July 1977).

6. Memo, R. A. Wagner, RE/SPEC, Inc., to Dr. J. E. Russell and Dr. W. C. McClain, Office of Waste Isolation, dtd April 25, 1978, Subject: Considerations for the Calibration and Application of the Vibrating Wire Stressmeter in Salt.

7. H. E. Anderson, "STAT/LIB," Sandia Laboratories Report SAND74-0225, Albuquerque, NM, October 1974.

DISTRIBUTION

U.S. Department of Energy, Headquarters
Office of Nuclear Waste Management
Washington, DC 20545
- Eugene F. Beckett, Project Coordinator (WIPP) (1)
- Colin A. Heath, Director, Division of Waste Isolation (2)
- Sheldon Meyers
- Raymond G. Romatowski
- R. Stein
- Carl L. Cooley
- R. B. Chitwood

U.S. Department of Energy, Albuquerque Operations
P.O. Box 5400
Albuquerque, NM 87185
- D. T. Schueler, Manager, WIPP Project Office (2)
- G. Dennis, Director, Public Affairs Division
- S. C. Taylor, C&TI Division (for Public Reading Rooms)
- J. F. Bresson
- G. W. Johnson, Waste Management Branch

U.S. Department of Energy
Carlsbad WIPP Project Office
Room 113, Federal Building
Carlsbad, NM 88220

U.S. Department of Energy
c/o Battelle
Office of Nuclear Waste Isolation
505 King Avenue
Columbus, OH 43201
- Jeff O. Neff

Battelle Memorial Institute
Office of Nuclear Waste Isolation
505 King Avenue
Columbus, OH 43201
- Neil Carter, General Manager (3)
- R. Heineman
- Wayne Carbiener
- P. Hoffman
- R. Robinson
- G. Raines
- R. Cudnik
- S. Matthews
- ONWI Library

Westinghouse Electric Corporation
P.O. Box 40039
Albuquerque, NM 87196
- R. C. Mairson (3)

Hobbs Public Library
509 N. Ship Street
Hobbs, NM 88248
Ms. Marcia Lewis, Librarian

Lokesh Chaturvedi
Department of Civil Engineering
Box 3E
New Mexico State University
Las Cruces, NM 88003

Bechtel Inc.
P. O. Box 3965
San Francisco, CA 94119
R. A. Langley

National Academy of Sciences, WIPP Panel
Frank L. Parker, Chairman
Department of Environmental and
Water Resources Engineering
Vanderbilt University
Nashville, TN 37235

Konrad B. Krauskopf, Vice Chairman
Department of Geology
Stanford University
Stanford, CA 94305

Dr. Karl P. Cohen, Member
928 N. California Avenue
Palo Alto, CA 94303

Neville G. W. Cook, Member
Dept. of Material Sciences and Engineering
University of California at Berkeley
Heart Mining Building, #320
Berkeley, CA 94720

Merril Eisenbud, Member
Inst. of Environmental Medicine
New York University Medical Center
Box 817
Tuxedo, NY 10987

Fred M. Ernsberger, Member
Glass Research Center
PPG Industries, Inc.
Box 11472
Pittsburgh, PA 15238

Roger Kasperson, Member
Center for Technology, Environment and Development
Clark University
Worcester, MA 01610

Richard R. Parizek, Member
Department of Hydrogeology
Pennsylvania State University
University Park, PA 16802

Thomas H. Pigford, Member
Department of Nuclear Engineering
University of California
Berkeley, CA 94720

Roger W. Staehle, Member
Dean, Institute of Technology
University of Minnesota
Lind Hall
Minneapolis, MN 55455

John W. Winchester, Member
Department of Oceanography
Florida State University
Tallahassee, FL 32306

D'Arcy A. Shock
233 Virginia
Ponca City, OK 74601

National Academy of Sciences
Committee on Radioactive Waste Management
2101 Constitution Avenue, NW
Washington, DC 20418
John T. Holloway (2)

WIPP Public Reading Room
Atomic Museum, Kirtland East AFB
Albuquerque, NM 87185
Ms. Gwynn Schreiner

WIPP Public Reading Room
Carlsbad Municipal Library
101 S. Hallaqueno St.
Carlsbad, NM 88220
Lee Hubbard, Head Librarian

Thomas Brannigan Library
106 W. Hadley St.
Las Cruces, NM 88001
Don Dresp, Head Librarian

Roswell Public Library
301 N. Pennsylvania Avenue
Roswell, NM 83201
Ms. Nancy Langston

Bruno Giletti
Department of Geological Sciences
Brown University
Providence, Rhode Island 02912

Raymond Siever
Department of Geological Sciences
Harvard University
Cambridge, Massachusetts 02138

John Handin
Center of Tectonophysics
Texas A & M University
College Station, Texas 77840

John Lyons
Department of Earth Sciences
Dartmouth College
Hanover, New Hampshire 03755

George Pinder
Department of Civil Engineering
Princeton University
Princeton, New Jersey, 08540

New Mexico Advisory Committee on WIPP
NMIMT Graduate Office
Socorro, NM 87801
Marvin H. Wilkening, Chairman (2)

State of New Mexico
Environmental Evaluation Group
320 Marcy Street
P. O. Box 968
Santa Fe, NM 87503
Robert H. Neill, Director (2)

NM Department of Energy & Minerals
P. O. Box 2770
Santa Fe, NM 87501
Larry Kehoe, Secretary
Kasey LaPlante, Librarian

J. E. Magruder
Sandia Carlsbad Representative
401 North Canal Street
Carlsbad, NM 88220

Brookhaven National Laboratory
Associated Universities, Inc.
Upton, Long Island, New York 11973
Paul W. Levy, Physics Dept.

Dr. Paul R. Dawson
254 Upson Hall
Dept. Mech. & Aerospace Engr.
Cornell University
Itnaca, NY 14853

Fenix & Scisson, Inc.
401 N. Canal
Carlsbad, NM 88220

D. E. Maxwell
Science Applications, Inc.
2450 Washington Avenue, Suite 120
San Leandro, CA 94577

Oak Ridge National Laboratory
Box Y
Oak Ridge, TN 37830
Attn: R. E. Blanko
C. Clairborne

RE/SPEC Inc.
P. O. Box 725
Rapid City, SD 57701
Dr. P. Gnirk
L. Van Sambeek
R. Stickney

Mr. Michael J. Smith
Rockwell International
Atomics International Division
Rockwell Hanford Operations
P. O. Box 800
Richland, WA 99352

Systems, Science, and Software
Box 1620
La Jolla, CA 92038
E. Peterson

Billy J. Thorne, Vice President
Civil Systems Inc.
2201 San Pedro NE, Suite 214
Albuquerque, NM 87110

U.S. Geological Survey
P. O. Box 26659
Albuquerque, NM 87125
J. Mercer

U.S. Geological Survey
Special Projects
MS954, Box 25046
Denver Federal Center
Denver, CO 80255
C. Jones

Sandia Internal

1100 C. D. Broyles
1110 J. D. Plimpton
1112 C. R. Mehl
1116 S. R. Dolce
1116 E. S. Ames
1116 C. W. Cook (5)
1120 T. L. Pace
1125 G. L. Ogle
1125 J. T. McIlmoyle
1130 H. E. Viney
1133 R. D. Statler
2645 L. D. Bertholf
3141 T. L. Werner (5)
3151 W. L. Garner, For: DOE/TIC (Unlimited Release) (3)
3154-3 R. P. Campbell, For: DOE/TIC (25)
4500 E. H. Beckner
4510 W. D. Weart
4511 D. W. Powers
4512 T. O. Hunter (5)
4512 C. L. Christensen
4512 D. R. Fortney
4512 M. A. Molecke
4514 M. L. Merritt
4530 R. W. Lynch
4537 L. D. Tyler
4538 R. C. Lincoln
4540 M. L. Kramm
4541 L. W. Scully
4541 H. C. Shefelbine
4542 Sandia WIPP Central Files (2) (TSI)
4543 R. R. Beasley
4543 J. R. Tillerson
4700 J. H. Scott
4730 H. M. Stoller
4732 D. A. Northrop
4732 D. E. Munson
4732 A. R. Sattler
4733 C. L. Schuster
4738 J. R. Wayland
5511 D. F. McVey
5520 T. B. Lane
5521 R. D. Krieg
5530 W. Herrmann
5531 S. W. Key
5532 B. M. Butcher
5532 L. W. Teufel
5532 W. R. Wawersik